PPPL-3194 - Preprint: July 1996, UC-420, 421, 426

Tritium Recycling and Transport in TFTR Plasmas with Deuterium Neutral Beam Injection

R.V. Budny, M. Bitter, H.H. Duong,[a] Q. Gao,[b] D. Jassby, L.C. Johnson,[c] S. von Goeler, A.T. Ramsey, C.H. Skinner, and D.P. Stotler

Princeton University
Plasma Physics Laboratory
P. O. Box 451, Princeton NJ, 08544

PSI Conference, May 20-24, 1996

Abstract

Tritium recycling rates and transport into the reacting core of TFTR discharges heated with deuterium neutral beam injection are studied. The measured neutron emission rates and the TRANSP plasma analysis code are used. A model for the transport of tritium and deuterium is shown to simulate the DT neutron emission profile shapes in approximate agreement with measurements. The fraction of tritium in the hydrogenic recycling influx through the last closed flux surface is adjusted to fit the magnitude of the measured DT rates. This fraction is approximately 2-4 times the fraction of tritium in the Balmer-alpha line emission. Approximately 150 discharges are studied, including supershots, reversed shear and enhanced reversed shear discharges, H-mode discharges, and L-mode discharges. General scaling relations are given for the central tritium density, tritium recycling fraction, the global DD and DT neutron emission rates, and the tritium effective fueling efficiency at the time of peak DT neutron emission.

[a]General Atomics, ORAU Fellow, presently at Princeton Plasma Physics Laboratory.

[b]Southwestern Institute of Physics, Sichuan, P.R. China.

[c]Joint ITER Design Team, San Diego, CA.

1. Introduction

Fusion reactors will need to operate with approximately equal deuterium and tritium concentrations to optimize their fusion power. Especially if the plasma radii are large, it could prove challenging to fuel reactors with optimal concentrations. Also, since it is difficult to reprocess tritium, it will be important to fuel the tritium efficiently.

In present tokamak experiments, recycling from the walls is a significant source of fueling. In many tokamaks, it has been observed that when the recycling rates are large, the plasma performance (measured for instance by energy confinement or neutron emission) is degraded. Even in the highest performance TFTR supershots, which are produced by reducing the limiter recycling, the hydrogenic recycling rates (defined by the ionization rates within the last closed flux surface) are comparable to, or greater than the total beam fueling rates [1]. In order to control plasma performance it is important to quantify the recycling.

The aim of this paper is to study tritium recycling and transport in TFTR discharges whose only source of tritium is recycling from the walls. Neutral tritium is emitted from the walls, ionizes in the edge, is transported into the core, and recycles back out into the scrape off. The tritium density in the reacting core is indicated by the DT neutron emission profile. We show that the ionization rate within the last closed flux surface and the transport into the core can be modeled with the TRANSP plasma analysis code [2], achieving approximate agreement with the neutron measurements.

Typically, in modeling TFTR discharges, the hydrogenic recycling ionization rates are derived from the measured Balmer-alpha line emission using a conversion calculated with the DEGAS neutrals code [3-4]. There are considerable uncertainties in the DEGAS modeling due to the lack of detailed edge temperature and density measurements, so it is desirable to have independent checks of the results.

This paper uses a new technique of finding the fraction of tritium to hydrogenic recycling rates using neutron emission rates, which are measured with considerable accuracy. The results for this fraction are compared with the fraction of tritium in the Balmer-alpha line emission measured using a Fabry-Perot (FP) spectrometer [5]. The two techniques are consistent, within the uncertainties.

A wide range of TFTR discharges are studied. Section 4 gives scaling relations for the central tritium density, the fraction of tritium in the recycling, the DD and DT neutron emission rates, and the effective tritium fueling efficiency in terms of other plasma parameters measured at the time of peak DT neutron emission. Section 5 compares this tritium fraction with the fraction of tritium Balmer-alpha emission.

2. TRANSP modeling

TRANSP is used to model the time evolutions of plasma parameters. The energy, particle, and magnetic field dynamics are computed. Measured plasma profiles are used. Typically, measurements of the electron temperature (from electron cyclotron emission) and of the temperature and toroidal rotation velocity of the trace carbon impurity (from neutral-beam induced charge-exchange recombination spectroscopy) are inputs.

Several methods can be used to calculate Z_{eff}. These include using the visible bremsstrahlung (VB) emission along a chord passing near the plasma center, the Abel inverted VB emission profile, or the carbon density measured by charge-exchange recombination spectroscopy. The values calculated for Z_{eff} from these different approaches are in approximate agreement in the plasma region where most of the fusion reactions occur. For consistency, the first technique is used in this paper. The results are not very sensitive to the profile of Z_{eff}.

Hydrogenic Mixing - The total thermal hydrogenic density is determined in TRANSP from Z_{eff}, the beam modeling, and quasi-neutrality. The relative H, D, and T densities are calculated by choosing a hydrogenic mixing model which can be specified by several choices. The choice used here imposes constraints on the explicit radial diffusivities D_j and pinch velocities V_j. These define the radial fluxes Γ_j by

$$\Gamma_j = - D_j \ \mathrm{grad}(n_j) + V_j \ n_j \qquad (1)$$

with j = thermal H, D, or T. Proportionalities among the D_j and V_j can be set by the user. The V_j profiles are adjusted in time by TRANSP for each species so that Γ_j satisfy quasi-neutrality.

Naive prescriptions for the D_j and V_j coefficients do not simulate the DT neutron emission accurately. Since the hydrogenic mixing model specifies the tritium profile, and thus the DT neutron emission profile, it can be tested by comparing with measurements. The chordal DT neutron emission rates are measured along chords that pass vertically through the plasma [6]. Typically four or five chords traverse the region where the reactivity is high. Fig. 1 shows the simulated chordal emission using a naive prescription where D_j and V_j are the same for each hydrogenic species in the case of a supershot with plasma current I_p = 2 MA, major radius R = 2.52m, and the neutral beam injection (NBI) power P_{NB} stepped down. The time evolutions of the simulated profiles do not agree with the measured evolutions, which are also shown.

TRANSP achieves more accurate simulations if the values of D_j in the reacting core are large enough for the V_j to also be large in magnitude, and if V_T is reduced relative to V_D. In the following we assume constant and equal values for D_j, and that the V_j profiles are inversely proportional to the hydrogenic atomic mass A_j:

$$D_j = 1 \ \mathrm{m}^2 / \mathrm{sec}$$
$$V_j \propto A_j^{-1}. \qquad (2)$$

Our results do not depend sensitively on the profiles of D_j as long as their magnitude is sufficiently large in the reacting core.

The DT chordal neutron emissions simulated using the prescription (2) are compared in Fig. 2-a. One parameter, the fraction of tritium in the hydrogenic recycling, f_T, discussed later, is adjusted to set the scale of the simulations. The simulations are in approximate agreement within the measurement uncertainty which is ± 20%.

The simulated and measured global neutron emission rates are compared in Fig. 2-b. The global DT rate S_{DT} is measured using surface barrier detectors [7]. The total neutron emission rate is measured using a system of fission detectors [8]. The DD emission rate S_{DD} is gotten by subtraction. Generally when the TRANSP modeling gives good agreement with the S_{DT} rate, it also gives good agreement with the DT neutron emission chordal profile, and conversely.

The S_{DD} rate is simulated in TRANSP with no adjustable parameters. The simulations tend to be lower than the measurement by ≈ (0-20%). This discrepancy could be caused by systematic errors in the Z_{eff} or in the neutron emission rate measurements.

There is a theoretical indication that the isotopic dependence $V_j \propto A_j^{-1}$ is plausible. Three-dimensional global gyrokinetic particle simulations of ion temperature gradient drift instabilities in toroidal geometry predict anomalous inward particle pinches for trace ions [9]. These pinches result from the parallel acceleration and the E x B advection. The former gives rise to a Z / A dependence.

The choice of constraints (2) is not unique, and it is clear that alternative choices could give similar agreement with measurements. Since this paper studies tritium recycling and transport empirically, any prescription that gives the tritium profile consistent with the measurements is sufficient. A different empirical solution has been derived for D_T and V_T from discharges with brief puffs of tritium gas [10]. In that paper D_T increases with radius. The shape of V_T is similar in shape to the solutions computed by TRANSP using (2) during steady state phases of discharges.

The quantities that directly affect the particle conservation are Γ_j, not D_j and V_j. We have not found a prescription for constraining Γ_j that leads to accurate simulations of the DT neutron emission. The constraints for H are especially difficult to determine empirically since they do not participate in the fusion reactions. The specification of the H transport (2) is chosen by extrapolation of the D and T choices. The results reported here do not depend sensitively on this choice.

Recycling - The recycling sources are specified as the H, D, and T ionization rates I_j within the last closed flux surface. These are obtained from the measured Balmer-alpha line emission using conversions k_j derived using DEGAS. This DEGAS modeling gives k_j in terms of a conversion from photon rates to ionization rates, and a screening factor for the fraction of the ionizations that occur within the last closed flux surface. The screening factor is roughly 0.5. Their product k_j depends on plasma conditions, but is approximately constant to within a factor of three [1]. Since DEGAS results have large uncertainties, and are not available for many TFTR discharges, the k_j are held fixed at a nominal value, k. Sensitivity and variations are discussed in Section 7.

The h_α = $(H+D+T)_\alpha$ intensity is measured along five chords at one toroidal location. The ratios H_α / h_α and T_α / h_α are measured along one chord on the midplane using the FP interferometer. For this paper, the derived total (H+D+T) ionization rate (within the last closed flux surface) is partitioned into the H, D, and T ionization rates by specifying relative fractions, i.e.,

$$I = I_H + I_D + I_T = k\, h_\alpha \qquad (3)$$

$$I_j = f_j\, I$$

with $f_H + f_D + f_T = 1$. These relative fractions are held constant during each discharge.

The value of f_H for each discharge varies and is estimated from measurements of the ratio H_α / h_α. The range of values is typically (10-30)%. The results in this paperdo not depend sensitively on this input. The value of f_T is adjusted in iterations of TRANSP runs to match the magnitude of the DT neutron emission. The modeling is highly sensitive to this value. It is in the range < 10% for the discharges studied here. In the last section, the TRANSP f_T values are compared with the FP measured ratio T_α / h_α.

The TRANSP results for the particle fluxes can be used to compute the recycling coefficients R_j at the last closed flux surface defined as the ratios of the recycling sources divided by the out fluxes. These coefficients evolve during the discharge. For the discharge shown in Figs. 1-2, the recycling coefficients are $R_D \approx 0.7$ and $R_T \approx 1.0$ during the steady state phase.

3. Discharges Studied

The plasmas used for this study consist of most of the discharges with D-only NBI since the start of the DT experimental campaign (in December 1993) that have been modeled accurately with TRANSP. Modeling results are generally in approximate agreement (~ 2σ) with available measurements, at least through the time of peak neutron emission. A database of approximately 150 discharges was constructed incorporating plasma parameters at the time of peak S_{DT}, which is generally 0.5 - 0.7 sec after the start of the NBI, and generally after the times of peak total energy and of peak S_{DD}. All the discharges had extensive diagnostic coverage, including T_i and v_{phi} measurements.

Since the waveforms for S_{DD} are derived by subtracting S_{DT} from the total emission rate, the errors can be large when S_{DT} / S_{DD} is large. We concentrated on discharges with S_{DT} / S_{DD} < 3 to have accurate values for S_{DD}. Our results are insensitive to S_{DT} / S_{DD} up to this limit. A side effect of this constraint is an upper limit on the central tritium density ($6 \times 10^{17}/m^3$) and on f_T (9%).

Three categories of discharges are excluded from this study: 1) Discharges with major disruptions have S_{DT} increasing up to the time of the disruption, which occurs before comparable non-disruptive discharges obtain their peak S_{DT}. 2) Discharges with large amounts of He are not modeled accurately due to uncertanites modeling the He concentration. 3) Discharges with brief tritium puffs are excluded, although they are modeled accurately using the hydrogenic mixing model (2) by postulating an additional tritium ionization rate δI_T corresponding to the puff. The time integral of δI_T is typically 10% of the amount of tritium in the gas puff.

Types of discharges used in this study include supershots with varying degrees of conditioning, poorly conditioned (~ L-mode) discharges, discharges with ICRF in addition to the NBI, discharges for which the plasma current was ramped down, and discharges with reverse shear (RS) and with enhanced confinement and RS (ERS). We exclude these discharges from the scaling relations presented in the next section, but discuss qualitatively their scaling in the last section. The ranges of plasma parameters for the discharges studied are listed in Table I.

4. Results

Heuristic arguments can be used to relate the neutron rates with the central tritium, deuterium, and electron densities (n_T, n_D, n_e), and with I_T. Ignoring for the moment the important differences between the thermal and fast deuterium ions, and assuming that $n_T \propto I_T$, then $S_{DD} \propto n_D\, n_D$ and $S_{DT} \propto n_D\, n_T$ implies

$$n_T \propto n_D\, S_{DT} / S_{DD} \tag{4a}$$

$$S_{DT} \propto S_{DD}^{0.5}\, I_T \tag{4b}$$

A more useful version of (4a) results from the fact that during the steady state phases of TFTR discharges, the central Z_{eff} and the ratio of n_D / n_e are approximately constant. Thus

$$n_T \approx C\, n_e\, S_{DT} / S_{DD} \tag{4c}$$

The variation of the right side of (4c) has been explored in sequences of similar discharges with D-only NBI [11]. It decreases systematically with the number Δ of NBI-heated discharges since the previous DT discharge approximately as $\Delta^{-0.45}$.

We use regression of the database to study relations among plasma parameters. Regression confirms (4c) with C = 0.003 ± 0.001. There is a weak plasma current dependence ($I_p^{-0.11}$). The central tritium density (m^{-3}) and f_T are related as:

$$n_T \approx 2.6\text{x}10^{20}\ f_T^{1.0}\ V_p^{-1.0}\ I_p^{0.23} \tag{5a}$$

$$f_T \approx 1.4\text{x}10^{-3}\ (S_{DT} / S_{DD})^{0.96}\ P_{NB}^{0.18}\ V_p^{0.6} \tag{5b}$$

with V_p the plasma volume (m^{-3}), P_{NB} in MW, and I_p in MA.

Regression gives a scaling relation for the DD neutron emission rate (/s) as

$$S_{DD} \approx 6.6\text{x}10^{6}\ E^{1.81}\ V_p^{-0.83}\ I_p^{0.50}\ B_T^{0.22} \tag{6a}$$

where E is the total energy (MJ), and B_T is the toroidal field (T). A plot of the fit versus S_{DD} is shown in Fig. 3.

A wide range of plasma conditions are fitted by (6a). Three categories of discharges are indicated in Fig. 3. These are discharges with the current ramped down during the NBI phase, and discharges with constant current, separated according to whether their total energy confinement is greater or less than 1.5 times the Goldston L-mode scaling value [12]. Some of the discharges had extensive Li conditioning. Many had a variety of MHD activity such as sawteeth or coherent modes. Some experienced beta collapses, minor disruptions, or impurity blooms near the time of peak S_{DT}. The ratios of the fit to the measured S_{DD} do not show a dependence on the major radius R, I_p, $q_\psi(a)$, B_T, P_{NB}, or S_{DT} / S_{DD}.

It is noteworthy that (6a) gives an accurate fit without invoking an explicit dependence on recycling parameters (such as h_α or the CII line emission). The total energy E does depend sensitively on recycling parameters.

The scaling (6a) is similar to a fit published previously [13]. For that study, based on a more narrow range of plasma conditions, the V_p dependence was forced to be V_p^{-1} and a weak dependence on $q_{cycl}(a)$ was found. An alternative fit to S_{DD} has a similar q dependence.

In Reference [13], the DT neutron emission from plasmas with DT-NBI was shown to obey a similar scaling as D-only NBI plasmas, but with magnitudes higher by a factor of ~ 130. A fit for S_{DT} in the D-only NBI discharges considered here is given by

$$S_{DT} \approx 3.6\mathrm{x}10^{10}\, E^{1.52}\, V_p^{-1.49}\, I_p^{0.30}\, f_T^{0.97} \tag{6b}$$

A plot of this fit versus S_{DT} is shown in Fig. 4. It has a similar E dependence as (6a), but a more rapid decrease in V_p. There could be an artificial V_p scaling introduced by the assumption that k_i is constant. This is discussed in the next section.

A measure of the effective tritium fueling efficiency is given by the ratio S_{DT} / I_T. The computed ratio is $(3 \pm 2)\mathrm{x}10^{-4}$. Thus most of the tritium ions recycle out of the last closed flux surface without fusing. This effective fueling efficiency increases with plasma performance, the electron density peakedness, V_p, and I_p.

5. Discussion

Discharges with reversed shear were excluded from the regression fits and plots above. They obey the S_{DD} fit (6a), but their scaling in S_{DT} are (0-20%) lower than the fit (6b). They all have large major radii (~2.6m). There is uncertainty in the measured h_α for plasmas with large radii since the chords view the inner limiter, whereas the large plasmas may experience recycling on the outer walls. Other types of discharges with large radii have S_{DD} and S_{DT} scaling relations consistent with those of discharges with intermediate radii (2.5m) and small radii (2.45m).

The DEGAS modeling has not been done for many discharges, so a nominal k_j value was used in this study. There are considerable uncertainties in the DEGAS modeling. The scrape off plasma parameters need to be specified to model the interactions of the recycling neutrals. These parameters are gotten by extrapolating the edge values from the TRANSP modeling, which are not known accurately. The scrape off decay lengths are adjusted to fit the measured poloidal profiles of the h_α emission.

The DEGAS values for the k_j tend be (1-3) times the nominal value used here. They tend to increase as the major radius of the plasma increases since larger plasmas have smaller scrape off volumes in which recycling neutrals can be ionized. Also k_j decrease with the hydrogenic isotopic mass since the velocity of the neutrals decreases with A. This mass effect also causes the poloidal profiles of I_T to be shifted away from the midplane, relative to I_D.

Measurements of T_α / h_α from the FP spectrometer are available for some of the discharges studied here. The TRANSP results for f_T are higher by a factor of (2-4). Several effects could be causing this: 1) The f_T fits are global values since the TRANSP modeling and the neutron measurements do not depend on toroidal or poloidal variables, whereas the FP measurements are along one chord viewing the midplane. There is a strong poloidal variation of h_α with a minimum at the midplane. The tritium embedded in the limiter is believed to depend on limiter regions as a consequence of the past plasma operating conditions (radii, DT-NBI, etc.). It is not known if the ratio of the tritium and deuterium particle recycling varies in location. 2) The nominal value of k used in this study is low compared with DEGAS results. If k is increased, the result for f_T that fits S_{DT} is reduced, giving better agreement. 3) As noted above, the radial profiles of the D and T Balmer-alpha emission and ionization rates are modeled to be different. The FP measurement integrates over this profile, whereas the TRANSP input integrates the ionization rate only to the last closed flux surface.

In summary, TRANSP can accurately model the DT neutron emission in a wide variety of plasma types with D-only NBI. A mass-dependent pinch velocity V_T is used, and the ratio f_T of tritium in the hydrogenic recycling is adjusted. The results for this ratio are consistent with the spectroscopic measurements, to within the experimental and modeling uncertainties. More DEGAS modeling is needed to confirm these comparisons.

Acknowledgments

We wish to thank M.G. Bell, D.K. Owens, S. Scott, J. Strachan, and M. Zarnstorff for helpful discussions, and the U. S. Department of Energy for support under the Contract No. DE-AC02-76-CH0-3073.

Table I - Ranges of plasma parameters

Parameter	Range
P_{NB} (MW)	4 - 30
P_{ICRF} (MW)	0 - 6
I_p (MA)	0.6 - 2.55
R_0 (m)	2.45 - 2.62
B_Z (T)	2 - 5.5
q_ψ (a)	4 - 26

References

[1] R.V. Budny and the TFTR group, J. Nucl. Mater. **176 & 177** (1990) 427.

[2] R. V. Budny, M. G. Bell, A.C. Janos, *et al.*, Nucl. Fusion **35** (1995) 1497, and referecnes therein.

[3] R. V. Budny, D. Coster, *et al.*, Jour. Nucl. Materials, **196-198** (1992) 462,

[4] D. Stotler, *et al.*, new paper.

[5] C.H. Skinner, H. Adler, R.V. Budny, *et al.*, Nucl. Fusion **35** (1995) 143.

[6] S. VonGoeler, A.L. Rockmore, L.C. Johnson, *et al.*, Rev. Scientific. Instruments, **67** (1996) 473.

[7] E. Ruskov, W.W. Heidbrink, *et al.*, Rev. Scientific Instruments, **66** (1994) 910.

[8] L.C. Johnson, C.W. Barnes, *et al.*, Rev. Scientific Instruments, **66** (1995) 894.

[9] R. Santoro, W. Lee, and S. Parker, private communication.

[10] P.C. Efthimion, L.C. Johnson, J.D. Strachan, *et al.*, Phys. Rev. Letters, **75** (1994) 85.

[11] S. Kruger, R.V. Budny, C. Skinner, and J.D. Strachan, Nucl. Physics, **36** (1996) ????.

[12] R. Goldston, Plasma Physics and Controlled Fusion, **26** (1984) 87.

[13] M.G. Bell, C.W. Barnes, R.V. Budny, *et al.*, Proceedings of the 15th International Conference on Plasma Physics and Controlled Nuclear Fusion Research, Seville, Spain, 1994. IAEA-CN-60/A-2-I-1.

Figure Captions

Fig. 1 Time evolutions of simulations using a naive choice of D_j and V_j (without an isotopic dependence), and the measured DT chordal neutron emission rates for a supershot.

Fig. 2 Time evolutions of the simulations using prescription (2), and measurements of a) the DT chordal neutron emission rates, and b) the DD, DT, and total neutron emission rates.The relative tritium fraction f_T = 0.037 was used.

Fig. 3 Comparison of the fit and measured S_{DD} at the time of peak S_{DT}.

Fig. 4 Comparison of the fit and measured S_{DT}.

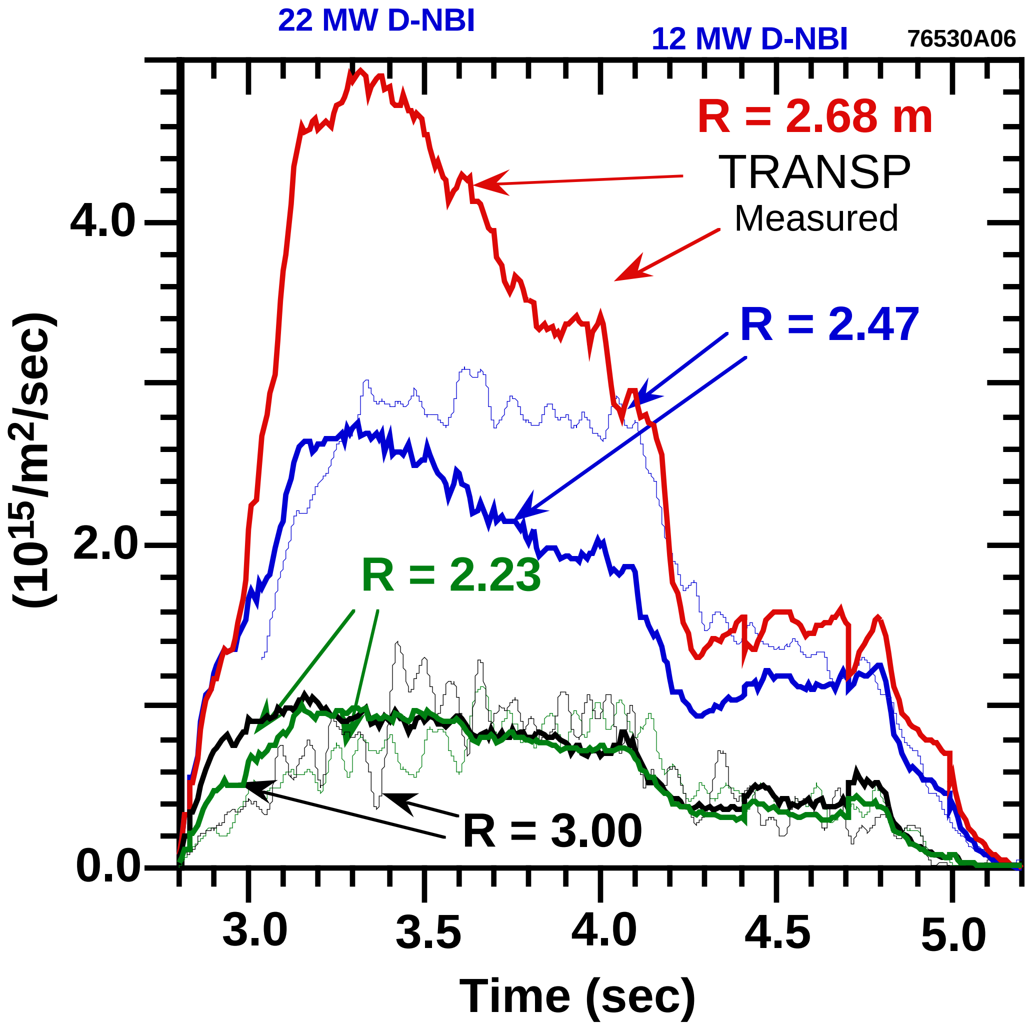
22 MW D-NBI
12 MW D-NBI
76530A06
R = 2.68 m
TRANSP
Measured
R = 2.47
R = 2.23
R = 3.00
4.0
2.0
0.0
(10^15/m^2/sec)
3.0
3.5
4.0
4.5
5.0
Time (sec)

Figure 1

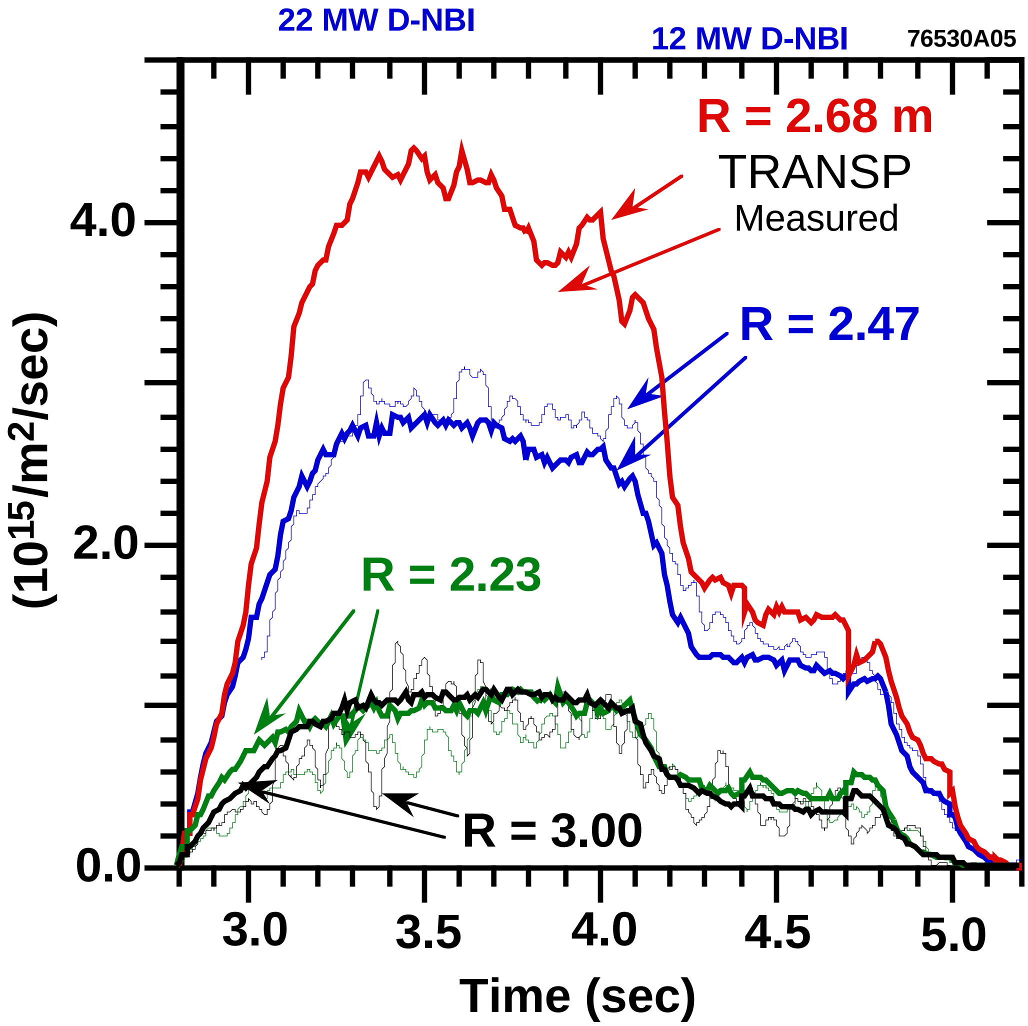
22 MW D-NBI
12 MW D-NBI
76530A05
R = 2.68 m
TRANSP
Measured
R = 2.47
R = 2.23
R = 3.00
4.0
2.0
0.0
(10^15/m^2/sec)
3.0
3.5
4.0
4.5
5.0
Time (sec)

Figure 2-a

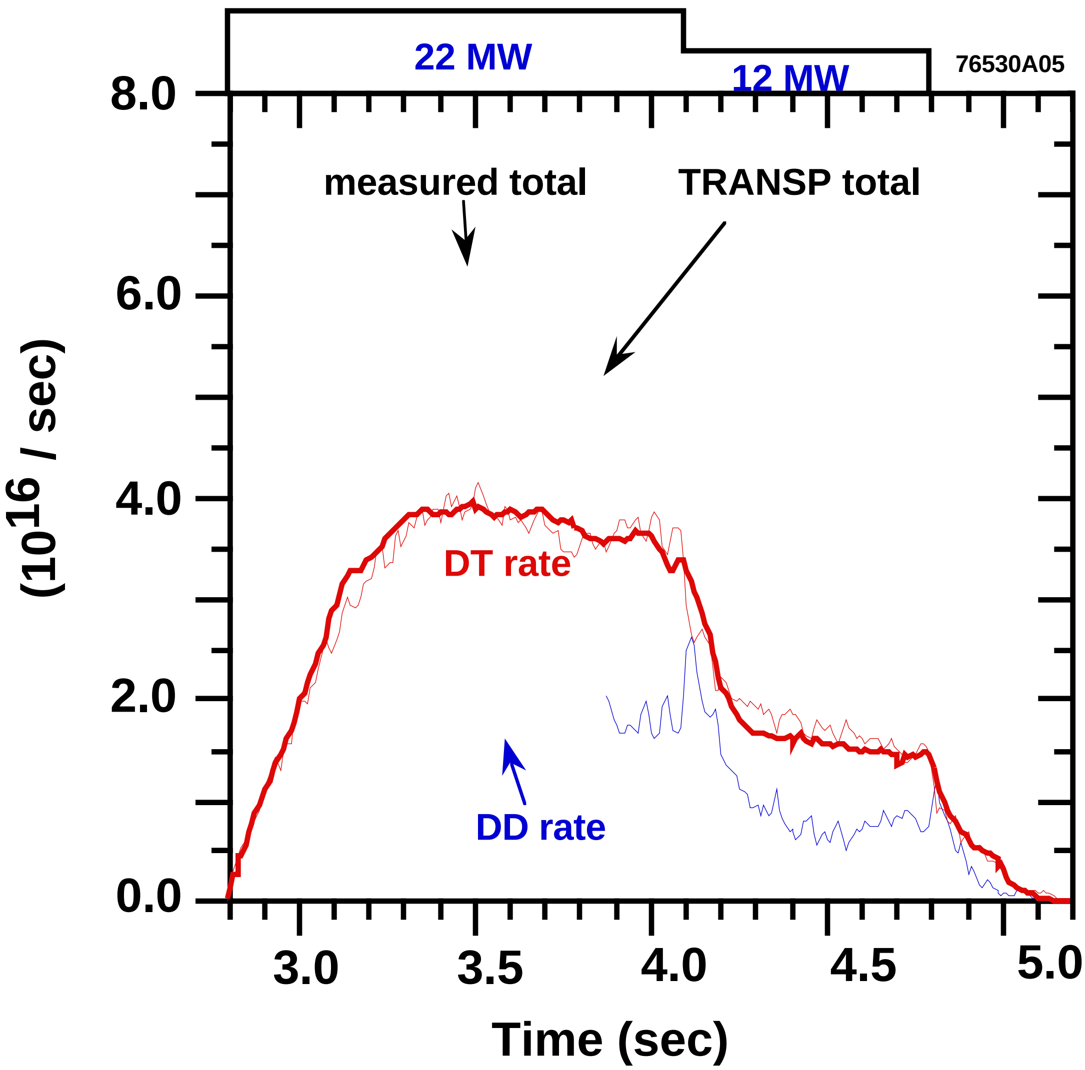

22 MW
12 MW
76530A05
8.0
6.0
4.0
2.0
0.0
measured total
TRANSP total
DT rate
DD rate
(10^16 / sec)
3.0
3.5
4.0
4.5
5.0
Time (sec)

Figure 2-b

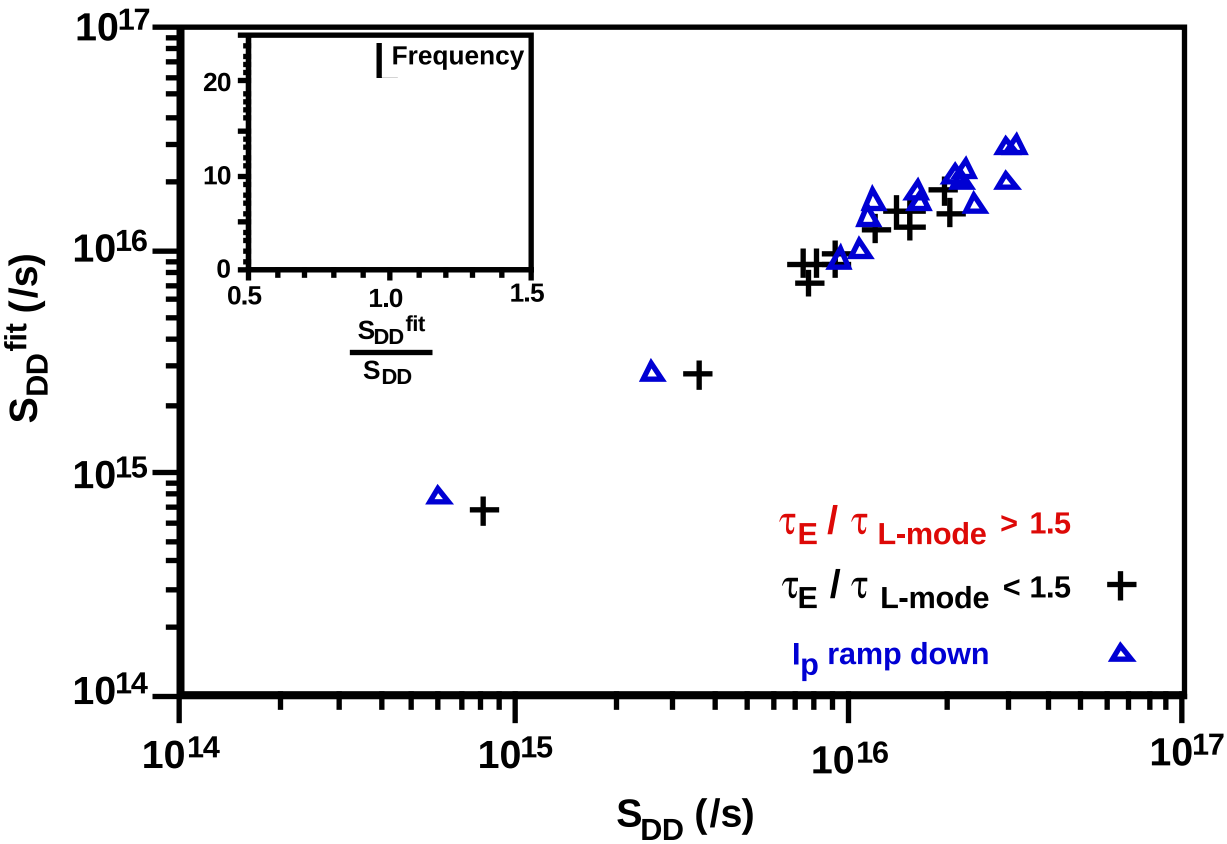

$$S_{DD}^{fit} = 6.6\mathrm{x}10^6\ E_{tot}^{1.8}\ V_p^{-0.8}\ I_p^{-0.5}\ B_T^{0.2}$$

Figure 3

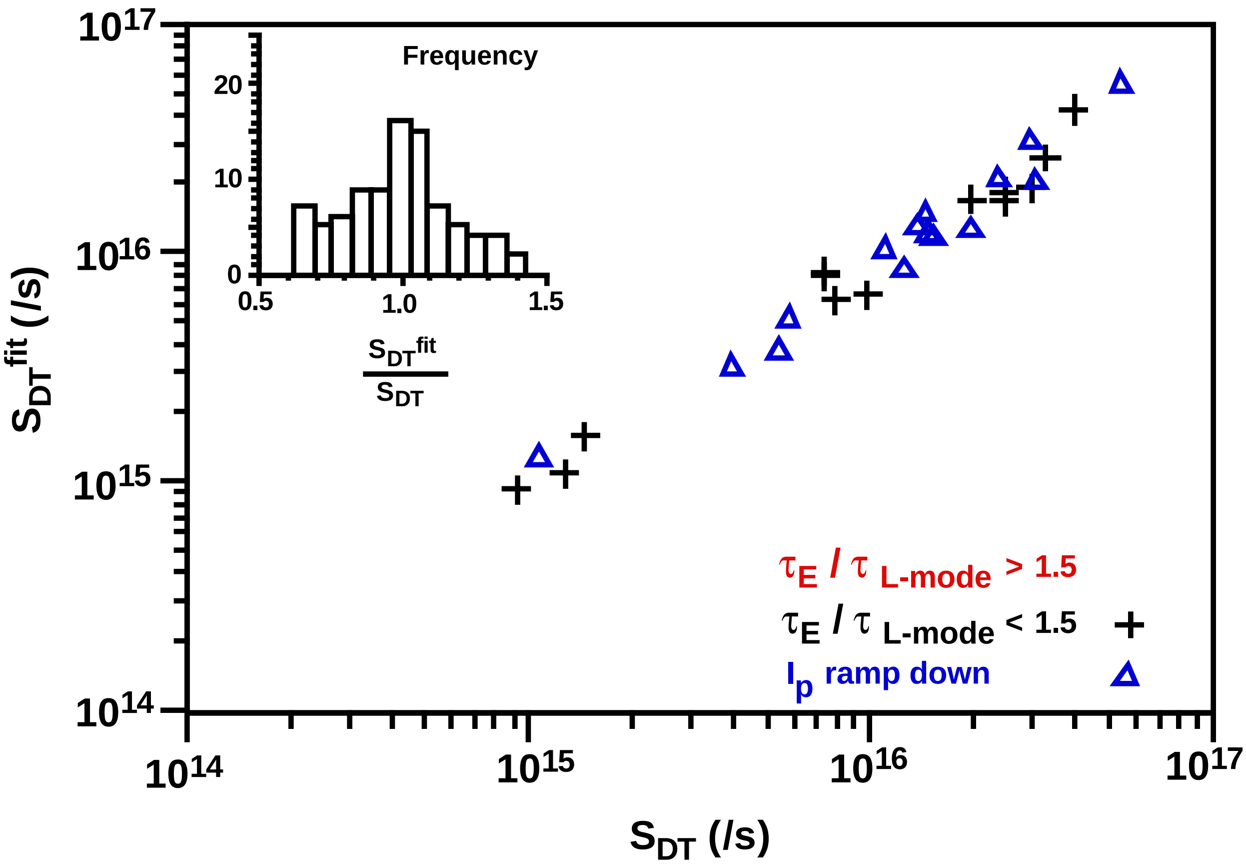

$$S_{DT}^{fit} = 3.1\text{x}10^{10}\ E_{tot}^{1.5}\ V_p^{-1.5}\ I_p^{-0.3}\ f_T^{1.0}$$

Figure 4